On-site construction of a point-of-care low-field MRI system in Africa

Obungoloch, Johnes; Muhumuza, Ivan; Teeuwisse, Wouter; Harper, Joshua; Etoku, Ivan; Asiimwe, Robert; Tusiime, Patricia; Gombya, George; van Gijzen, Martin; More Authors

DOI
10.1002/nbm.4917

Publication date
2023

Document Version
Final published version

Published in
NMR in Biomedicine

Citation (APA)
Obungoloch, J., Muhumuza, I., Teeuwisse, W., Harper, J., Etoku, I., Asiimwe, R., Tusiime, P., Gombya, G., van Gijzen, M., & More Authors (2023). On-site construction of a point-of-care low-field MRI system in Africa. *NMR in Biomedicine*, *36*(7), Article e4917. https://doi.org/10.1002/nbm.4917

Received: 7 November 2022 | Revised: 14 February 2023 | Accepted: 5 March 2023

DOI: 10.1002/nbm.4917

RESEARCH ARTICLE

NMR IN BIOMEDICINE WILEY

On-site construction of a point-of-care low-field MRI system in Africa

Johnes Obungoloch[1] | Ivan Muhumuza[1] | Wouter Teeuwisse[2] | Joshua Harper[3] | Ivan Etoku[1] | Robert Asiimwe[1] | Patricia Tusiime[1] | George Gombya[1] | Chris Mugume[1] | Mary Hellen Namutebi[1] | Mary Anthony Nassejje[1] | Maureen Nayebare[1] | Joseph Mark Kavuma[1] | Benedicto Bukyana[1] | Faith Natukunda[1] | Patience Ninsiima[1] | Abraham Muwanguzi[4] | Phillip Omadi[4] | Martin van Gijzen[5] | Steven J. Schiff[6] | Andrew Webb[2] | Tom O'Reilly[2]

[1]Department of Biomedical Engineering, Mbarara University of Science and Technology, Mbarara, Uganda

[2]Department of Radiology, Leiden University Medical Center, Leiden, The Netherlands

[3]Universidad Paraguayo Alemana, San Lorenzo, Paraguay

[4]Ugandan National Planning Authority, Kampala, Uganda

[5]Delft Institute of Applied Mathematics, Technical University of Delft, Delft, The Netherlands

[6]Department of Neurosurgery, Yale University, New Haven, Connecticut, USA

Correspondence
Andrew Webb, Department of Radiology, Leiden University Medical Center, 2333 ZA Leiden, The Netherlands.
Email: a.webb@lumc.nl

Funding information
European Commission; National Institutes of Health, Grant/Award Number: 2R01HD085853; Nederlandse Organisatie voor Wetenschappelijk Onderzoek

Purpose: To describe the construction and testing of a portable point-of-care low-field MRI system on site in Africa.

Methods: All of the components to assemble a 50 mT Halbach magnet-based system, together with the necessary tools, were air-freighted from the Netherlands to Uganda. The construction steps included individual magnet sorting, filling of each ring of the magnet assembly, fine-tuning the inter-ring separations of the 23-ring magnet assembly, gradient coil construction, integration of gradient coils and magnet assembly, construction of the portable aluminum trolley and finally testing of the entire system with an open source MR spectrometer.

Results: With four instructors and six untrained personnel, the complete project from delivery to first image took approximately 11 days.

Conclusions: An important step in translating scientific developments in the western world from high-income industrialized countries to low- and middle-income countries (LMICs) is to produce technology that can be assembled and ultimately constructed locally. Local assembly and construction are associated with skill development, low costs and jobs. Point-of-care systems have a large potential to increase the accessibility and sustainability of MRI in LMICs, and this work demonstrates that technology and knowledge transfer can be performed relatively seamlessly.

KEYWORDS
Accessibility, halbach magnets, low field MRI, open-source spectrometer, point-of-care MRI, sustainable design

Abbreviations: 3D, three dimensional; CNC, computerized numerical control; LUMC, Leiden University Medical Center; MUST, Mbarara University of Science and Technology; PMMA, polymethylmethacrylate.

Johnes Obungoloch, Ivan Muhumuza, Wouter Teeuwisse, Joshua Harper, and Ivan Etoku made joint first author contributions.

1 | INTRODUCTION

The lack of MRI facilities, both clinical and research, in the African continent has been highlighted in several recent articles.[1–3] A recent publication both outlines the current situation and proposes plans for improving this situation in the future.[2] Four crucial challenges were highlighted: access and availability, personnel training and education, research capacity and sustainable technology. One approach that can potentially address many of these recommendations is low-field MRI. If provided in the right way, it offers not only a way to rapidly increase the number of MRI scanners in the continent and the diversity of access to these scanners, but also a platform for teaching, education and research development. In order to fulfil these requirements, the system must be designed to be affordable, but equally importantly to be understandable and repairable by, for example, local medical physicists and/or electricians. Critically important is that knowledge, even if developed in well funded facilities, should be transferred locally so that future developments can occur on site[4,5] and that sites within Africa can become training centers to effectively disseminate the expertise throughout the subcontinent.

In September 2022, a team of researchers from the Netherlands and Paraguay worked with local students and professionals at the Mbarara University of Science and Technology (MUST) to construct, on site, the first custom-built point-of-care MRI system in Africa. Much of the development work had previously been performed outside Africa, with grants provided by the National Institutes of Health supporting the African engineering team and initially funding an earlier approach using electromagnets,[6] the Dutch National Science Foundation (NWO) enabling the development of a Halbach-based permanent magnet system,[7] and the European Research Council, which had supported the development of an open-source MRI spectrometer.[8] Funds from each of these entities were used to produce a "kit," which was shipped to Uganda. The build was carried out in parallel with "The first low-field Sub-Saharan Africa MRI training workshop," funded by the Chan Zuckerberg Initiative, in which students from Nigeria, Ghana, Uganda, Cameroon, Mozambique and South Africa attended lectures on basic MRI to provide additional context for the construction.

The specific application to which this project is targeted is to provide context appropriate brain imaging for treatment planning of infant hydrocephalus in Uganda. There are approximately 180 000 new cases of infant hydrocephalus in sub-Saharan Africa per year,[9] which represents a significant disease burden on the population. Each case requires surgical intervention and follow-up, making neuroimaging necessary. Low-field MRI could be an optimal imaging modality for this application based on the achievable image quality and local context.[6]

This contribution to the special edition on MRI accessibility does not represent a conventional scientific publication, but rather addresses the question of how one attempts, in a practical manner, to convert academic developments in the area of low-field MRI design and construction[7,10,11] into a practical product that can be manufactured and assembled on site, in this case in Uganda. Logistics, training, knowledge transfer, and infrastructural capabilities are the focus of this paper, rather than device optimization and design as in standard publications. We aim to give a realistic assessment of the challenges in transferring knowledge from high-resource to lower-resource environments. We note that the decision to ship the majority of the materials from the Netherlands was taken since we had only two weeks available for the entire build.

2 | METHODS

2.1 | Preparation, shipping and transportation

Prior to the travel of the visiting team and shipment of the components, the team in Leiden worked online to train the team at MUST on aspects of construction of Halbach magnet systems. Prototype designs were sent to the team in Uganda with instructions of how to three-dimensional (3D) print and assemble them. The team did this as a practice run and came up with a 10 cm Halbach system consisting of 3D printed rings. Some expertise and skills were developed in this process that turned out to be very useful in the fabrication of the bigger system. The laboratory had already constructed an open-source design 3D robot for mapping the B_0 field.[12]

In total about two months preparation time was necessary for all the components to be produced or ordered/delivered in the Netherlands. The delivery time for the computerized numerical control (CNC) plastic rings for the magnet was 3–6 weeks. Magnets were ordered from Supermagnete.nl, with the request that they all come from the same batch, and delivery times are between 4 and 8 weeks. The three gradient coil formers took about 60 days of 3D printing time in the Leiden laboratory, and so were printed in parallel on three different systems; no attempt was made to optimize printing time and so this might be reduced significantly. Tools, wire supplies, aluminum pieces for the cart and so on had a delivery time of a few days. PC boards for the MaRCoS system take about two weeks to deliver.

Figure 1 shows photographs of the major components of the system, which were shipped from Leiden via Schiphol Airport (The Netherlands) to Mbarara via Entebbe Airport (Uganda). All components, from custom machined or 3D-printed parts to nuts and bolts, from the gradient amplifier[13] to wire to wind the gradient coils, as well as the tools required to build the low-field scanner, were packed in a crate measuring 1.2 m × 1.0 m × 0.8 m with a total weight close to 325 kg. A full list of components as well as tools used for assembly is given in the Supporting Information. A forwarding company with a liaison agent in Uganda was hired for door-to-door handling and shipping at a price of around $2700 US. Since the build is not a commercial activity but rather part of a scientific cooperation between the Leiden University Medical Center (LUMC) and MUST, the shipment was eligible for tax exemption on import taxes. Both the application for tax exemption and that for customs clearance proved time consuming and took 6 and 2 weeks, respectively. However, upon reaching the airport, it was discovered that the shipment had also to be cleared

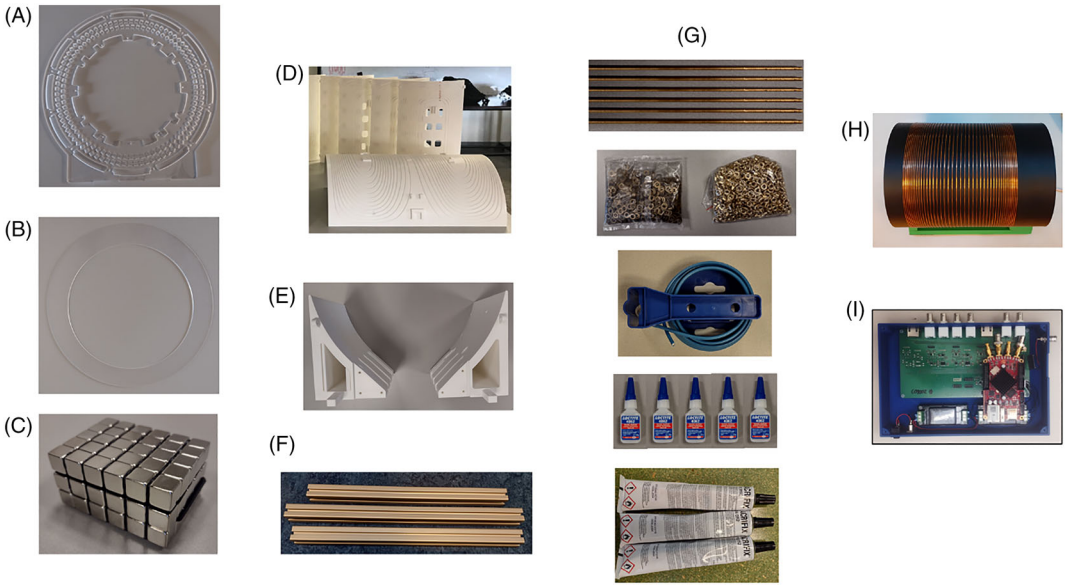

FIGURE 1 Photographs of the major components of the system. A, Plastic rings in which the individual magnet elements are placed; B, lids for each side of the rings; C, 12 × 12 × 12 mm^3 NdBFe magnets; D, 3D printed gradient coils with grooves for wire insertion; E, 3D printed supports for the finished magnet assembly; F, aluminum used for the trolley; G, small parts—brass rods/nuts/bolts/wire/superglue/PMMA glue; H, simple wire-wound solenoid coil; I, custom-built spectrometer based on a Red Pitaya.

FIGURE 2 Left, Crate containing all components including assembly tools, overall size 1.2 m × 1.0 m × 0.8 m and weight 325 kg. Center, Final delivery after two weeks en route, via taxi from the closest airport 5 h away. Right, Illustration of individual plastic rings for the magnet.

by the national standards body. It should be noted that some of the devices were components that did not have standards to conform to and the national standards body did not have standards against which they could be tested. This shows that, apart from developing the low-field MRI system in low-resource settings, there might also be need to help in the development of local standards.

The liquid glue used to fix the plastic lids onto the polymethylmethacrylate (PMMA) rings is considered a dangerous good and had to be shipped separately. Due to this classification transportation costs are high: $1100 US for a 4 kg package, of size 20 cm × 30 cm × 25 cm. These costs may be reduced if such materials can be ordered within the continent.

On a practical level one should bear in mind that facilities for delivery after shipping may be somewhat limited. As an example, the 325 kg crate was delivered with a van that could just accommodate it, as shown in Figure 2, and did not have a hydraulic lift. Since a fork lift was not available on site we ended up opening the crate in the back of the van at night and carrying out items one piece at a time into the laboratory. This underscores the need for more portable point-of-care technologies, to which the low-field MRI system developed conforms.

2.2 | On site facilities and resources

Electrical outlets were nominally 240 V, but experience large voltage swings throughout the day between about 210 and well above 250 V. In order to limit potential damage to sensitive equipment the local filtering and conditioning has an upper voltage clamp at 250 V. Every day there was at least one shutdown of power, in which case a backup generator would usually power up within about 10 s, although this was unavailable in the evenings and at weekends.

2.3 | Magnet construction

The shipped components for magnet construction were 25 PMMA rings produced via a CNC mill, M4 and M5 threaded brass rods (length 382 and 504 mm, respectively), brass nuts and washers (M3, M4, M5), 50 PMMA "lids" 2 mm thick for the magnet rings, glue, and 4089 12 × 12 × 12 mm^3 NdFeB N-48 magnets. Technical details of optimization of magnet orientations and placements have been published previously.[14] Due to the brittle nature of the PMMA and the lack of experience of working with this material amongst the assembly crew in Uganda we also included a spare copy for each unique ring design (13 in total) and 10 spare lids to ensure that any breakage would not lead to construction delays. Similarly, since the individual magnets are easily damaged (if they collide with one another the nickel coating is quite susceptible to cracking, and if this happens then the adhesive between the coating and the magnet often cracks the magnet as well) and may come with defects, a total of 4320 magnets were shipped to make allowances for rejecting unsuitable magnets.

Despite the lack of experience among the assembly crew, only one ring was damaged during preparation and had to be discarded. Approximately 60 magnets were rejected for visible, physical damage and fewer than 10 magnets were discarded for having field strength below specification.

It should be stated that for each step multiple independent quality checks were formally inserted into the build process and enforced regularly to ensure any mistakes were caught and fixed early on. Working with an inexperienced crew that included students, some of whom did not know anything about MRI prior, each step was preceded by a briefing and/or lecture delivered by a member of the visiting team explaining why it was important to follow instructions correctly.

Step 1: Magnets are typically shipped in a cubic arrangement, with plastic spacers in between. The first step is to permanently mark the north/south poles of the magnets. This is easily achieved by forming each box of magnets into a linear row, and then "sticking" them to a metallic surface, as shown in Figure 3. To ensure consistency a single magnet was pre-labelled according to polarity in the scanner at the LUMC. It was then packed in a layer of 3 mm transparent plastic and served as a reference when labelling the magnets for the new system.

Step 2: Any area of a ring that is glued to the lid, as well as the plastic lids themselves, are lightly hand sanded to aid adhesion. Any residual dust is cleaned off using a paper towel followed by an air blower.

Step 3: Filling each plastic ring with magnets. An easily identifiable landmark point should be made, for example the hole position where the axis of the magnet polarity is parallel to the ring radius. The first magnet is then placed, typically with the north pole of the magnet at the outside. Filling is performed by filling successive holes, which allows the first "sanity-check" that the magnet orientation is rotated by 180° when the magnet at one-quarter revolution is reached, by 360° at one-half, and by 180° at three-quarters. As each magnet is pulled off the linear stack, it is relatively easy to tell whether there is a "dud" magnet, which can be discarded. Typically we have found only about 1 in 1000 magnets to be of discernibly lower strength. For a more sensitive testing of individual magnets we used a make-shift setup consisting of an AlphaLab GM2 gaussmeter with the high stability probe with its field probe fixed inside a cardboard box lid that served as a guide for reproducible magnet positioning. After all of the magnets have been put in place, the field from each ring can be mapped by the robot. It is relatively easy from a two-dimensional scan to tell whether there is a sub-standard magnet, or if one has been inserted in the wrong orientation, as shown in Figure 4.

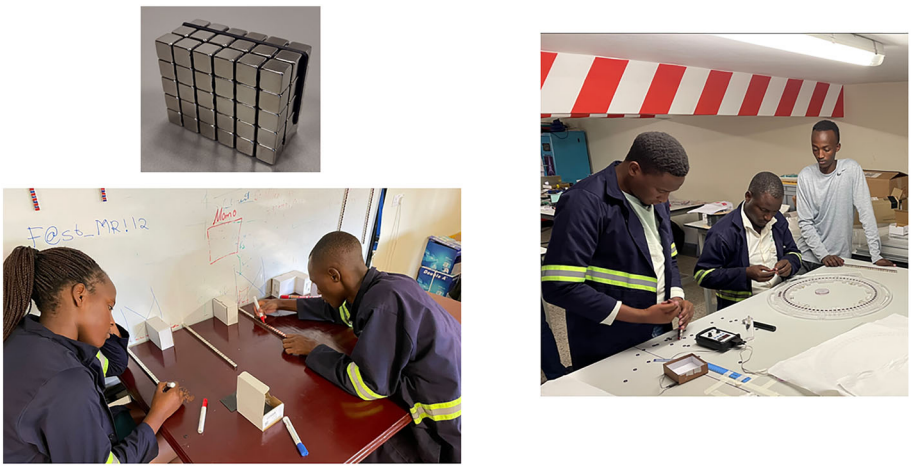

FIGURE 3 Individual steps in preparing the magnet components. Cubic magnets (upper left) are coloured to indicate north/south poles (lower left), and magnets are inserted manually into the holes in each ring (right).

Step 4: It is important that all of the magnets have been inserted to the same depth. This can be achieved by putting the ring on a very rigid flat table top and making sure that each magnet is pushed in till it touches the table top. When a ring is completely filled it is carefully placed on its side and held upright. We carefully checked that the face of all individual magnets is flush with the rear surface of the ring. This side of the ring is later used as reference for adjusting the ring-to-ring distance during assembly.

Step 5: For proper alignment of the lids 3D-printed clips are hooked onto three protrusions of the ring. With a 3D-printed comb the desired amount of PMMA glue (Acrifix 1R 0192) is smoothly spread onto the lid, which is then placed onto the ring. After the lid is in position and air bubbles are carefully pressed out, ring + lid are either placed into a UV box, or else can be placed in direct sunlight (approximate curing times are 17 min in a UV box, or a few hours in sunlight).

Step 6: After each ring has been solidly glued, the rings need to be arranged with very accurate spacing in between each pair of rings. Within the complete assembly of 25 rings three parts can be distinguished: a central part that consists of 17 rings with a larger inner diameter to create space for the gradient system, and two sets of three rings with smaller inner diameter that are first joined together to form a trio that is subsequently mounted on either side of the central part. The build is started by mounting 24 threaded rods (12 on the inside, 12 on the outside) onto the center ring, as shown in Figure 5. Nuts on either side of the ring are carefully adjusted such that each rod extends an equal distance from either side of the ring. Next the ring is positioned horizontally on an adequate support (Figure 5), nuts and washers are placed and the next ring is slid over the threaded rods and secured into place with washers and nuts. Taking the rear surface of Ring 1 as a reference, the distance to the rear surface of the second ring is measured and adjusted by turning the nuts on each of the 24 rods. Typical accuracies of 0.05 mm can be achieved using digital or analogue calipers.

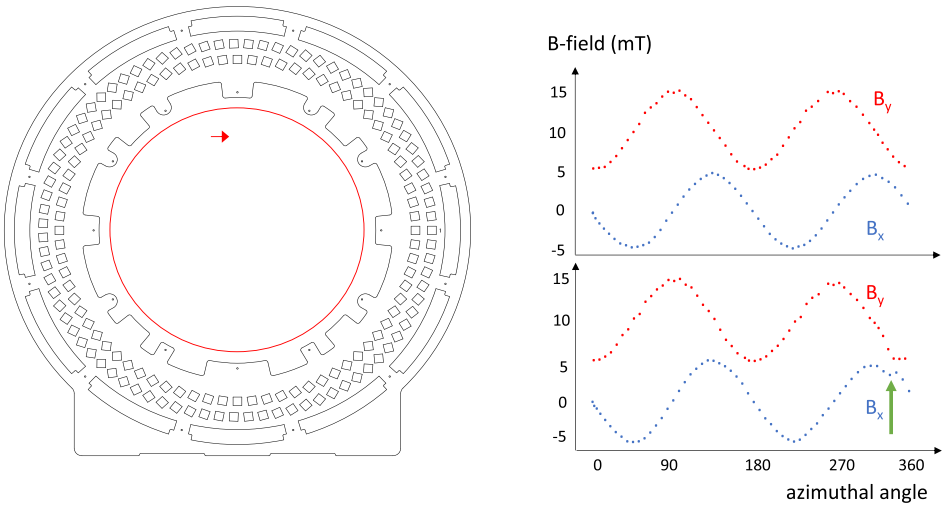

FIGURE 4 An example of *B*-field measurements made on each ring to check the orientation of each of the hundreds of magnets in each ring. The robot scans around the red line. The top plot on the right shows the expected sinusoidal variation in B_y and B_x fields as a function of azimuthal angle. In the bottom plot, one magnet has the incorrect polarity, which is shown by the green arrow.

FIGURE 5 Magnet assembly. Left, Brass rods are used to align each of the rings of the magnets. Nuts are used as spacers between each ring. The forces between the rings are significant but not dangerous. Center, After each ring is threaded onto the rods, the position of each nut is carefully adjusted so that there is equal spacing between each of the rings, and they are precisely aligned parallel to each other. Right, The completed magnet consisting of 25 rings, the central 17 containing two layers of magnets, and the front/back three rings having three layers.

2.4 | Gradient coils

Since the B_0 field of the magnet is transverse to its long axis, the design of gradient coils is slightly different from those familiar from conventional superconducting magnet designs. Different design methods, such as modified target field[10,15] or boundary element methods,[16] can be used. In our case we used the former method, available open source,[17] to obtain 3D wire patterns. These were then imported into the SolidWorks software package and output as STL files for 3D printing on polylactic acid (PLA) formers with thickness 5–6 mm and groove depth 2.7 mm such that coated 2.1 mm^2 wire could snugly be placed in the grooves. In order to facilitate modularity the inner *y*- and *z*-coils were fabricated in four different quadrants, with the outer *x*-coil fabricated as two halves, as shown in Figure 6. Approximate printing times using a Raise3D Pro2/3 Plus 3D printer were five or eight days per segment for the *Z*- and *Y*-gradient or *X*-gradient respectively. The total weight of all three gradient coils is approximately 8.5 kg.

In the laboratory in Uganda, the stages involved in producing the gradient coils were removal of residual plastic in the grooves (1.5 h per segment), placement of insulated wire and supergluing into place (1 h per segment), as shown in Figure 6.

When all formers are completed with wire *Z*-, *Y*- and *X*-gradient parts are mounted into place, which also involves installing the connecting wires and leads to the gradient amplifiers, as shown in Figure 7. After full assembly of the gradient coils, a copper sheet was formed in the center of the bore as an internal Faraday shield.

2.5 | B_0 field mapping

After placement of the RF shield, the final step in the construction, the B_0 magnetic field can be mapped using the previously mentioned robot (Figure 7). The AlphaLab GM2 magnetic field probe with the high stability probe has a usable resolution of around 5 μT and can be read out via USB allowing for an automated measuring setup. Shim trays containing smaller magnets can be added to improve the magnetic field homogeneity, if required, but this was not performed in this build due to time constraints. The trays in which the shim magnets can be placed were installed and two different sizes of shimming magnets (grade N42 $5 \times 5 \times 5$ mm^3 and grade N42 $6 \times 6 \times 6$ mm^3) were included in the crate. Once a B_0 map is acquired and shimming can be performed the individual shim magnet holders can either be 3D printed on site or shipped over.

FIGURE 6 Stages involved in gradient coil assembly from 3D printed formers. Left, Residual plastic from the 3D printing is removed to clear the grooves. Insulated wire is placed into the grooves and superglued into place after each turn. Right, Photograph showing one completed section: four sections are used for the two outer gradient sets, and two sections for the inner set.

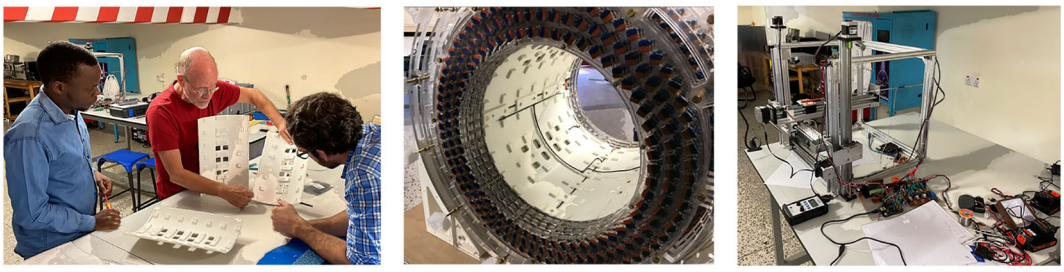

FIGURE 7 Installation of gradient set and system characterization. Left, The design consists of interlocking components, which click into place. Center, Before the final gradient set is inserted the wiring that connects the two halves and the gradient amplifier is installed. Right, After installation of the gradients a 3D robot is used to map the magnetic field.

2.6 | Aluminum trolley

The weight of the magnet plus gradient coils is approximately 125 kg. Since the system is designed to be portable, all of the electronic components with the exception of the spectrometer are designed to fit underneath the magnet. An aluminum trolley was constructed so that standard-sized components can be fitted into a 19 in. rack arrangement, as shown in Figure 8. In order to shield any electromagnetic interference (EMI) produced by the RF and gradient amplifiers, an aluminum plate is also placed on top of the trolley. A wooden surface is then placed on top of the aluminum plate. The 3D printed magnet holders are connected to this surface by drilling holes through the wood and screwing the holders into place to prevent the magnet from sliding.

2.7 | MR electronics

The MR spectrometer used to obtain initial images was the magnetic resonance control system (MarRCoS)[8] developed by a consortium of international researchers, details of which are available in open repositories.[18,19] MaRCoS is based on a Red Pitaya SDRlab, which includes an ARM processor, a Xilinx Zynq FPGA, two fast analog inputs, two fast analog outputs, and several digital input and output ports. The FPGA firmware (flocra) digitally controls the peripherals, such as RF transmit–receive chains and gradient coils. The ARM processor runs the MaRCoS server, which is the intermediate communication layer between the control computer and the FPGA. The control computer is equipped with a Python-based GUI, where pulse sequences can be programmed and executed. Sequences can be also programmed outside the GUI environment by writing them as text or NumPy arrays in Python, or in the Pulseq open-source framework.[20] Sequences on MaRCoS can also be directly programmed using the Python version of Pulseq.[21,22]

FIGURE 8 Construction of the portable trolley used for the system. Components consist of aluminum subunits screwed together.

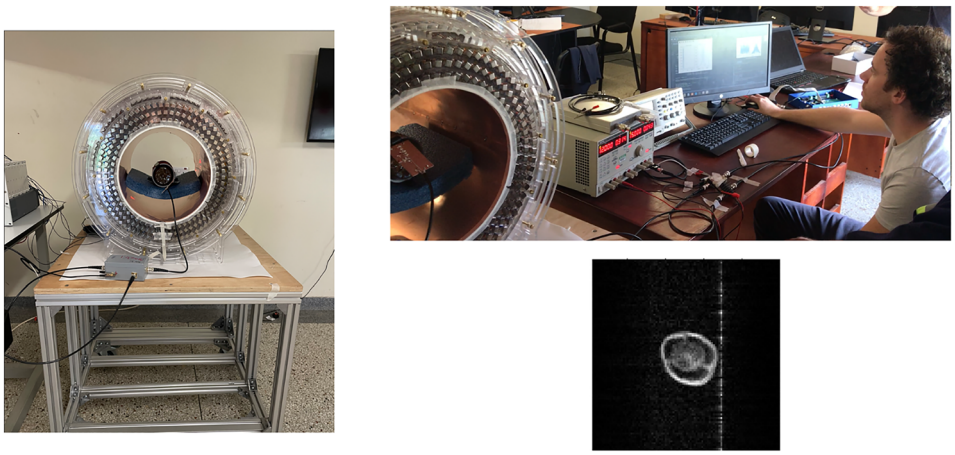

FIGURE 9 Completed system, with 10 cm diameter RF solenoidal coil placed in the center and a bell pepper used as the sample. A MaRCoS open-source spectrometer is used to acquire the data, with a small low-power Mini-Circuits amplifier used for the RF. Bottom right, The first image, showing a zipper artifact to illustrate that the data are real!

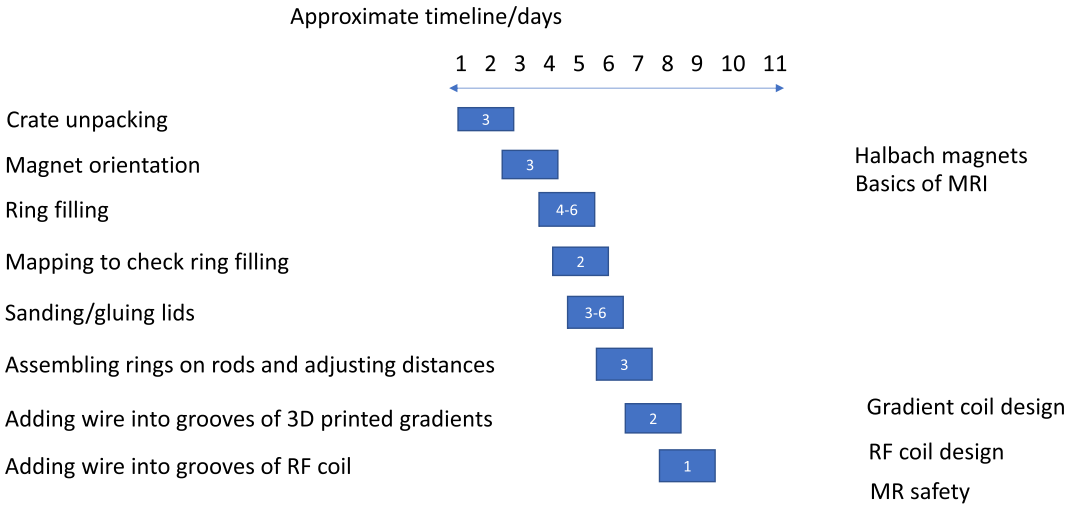

FIGURE 10 Approximate time-line for the build in Uganda, with four instructors and six students—work days were about 10 h per day with 1–2 h per day taken up by instruction. At each stage the approximate number of people working in parallel is indicated. On the right we outline the overall topics of lectures presented in parallel to the build.

The three-channel gradient amplifier is an open-source design[13] capable of providing up to about 15 A with a peak voltage of 13 V. For the small solenoidal coil, a low power RF amplifier can be used, in this case a Mini-Circuits ZX60-100VH+ with a maximum output power of 1 W. If more power is needed, that is, for in vivo imaging, then open source designs[23] with outputs up to 1 kW (gain of ∼54 dB) are available. The transmit–receive switch is a passive design based on a quarter-wavelength impedance transformer, implemented using a pi-network, and crossed diodes for switching between transmit and receive mode. A MITEQ preamplifier (AU-1054) with gain around 30 dB and noise figure around 1.2 dB was used for signal amplification. Figure 9 shows the completed magnet system with RF coil and associated electronics.

3 | APPROXIMATE TIMELINE

Figure 10 shows an approximate timeline for the build. This is intended as a guide, and should be reconciled with the fact that two instructors were present the entire time, with extensive experience of all aspects of the system construction. Six untrained persons performed the majority of the construction.

Compared with other systems in the literature, the only feature not installed currently is the particular form of shielding, except for a grounded copper sheet that lined the inside of the bore to prevent coupling between the RF and gradient coils. Many different types have been suggested in the literature, including a simple aluminum Faraday box[7] or flexible conducting cloth,[11,14,24] or the use of external sensors followed by signal processing to remove electromagnetic interference.[24,25]

4 | CONCLUSIONS

This work shows the feasibility and challenges associated with translating academic advances in point-of-care MRI to locations in which accessibility and sustainability are absolute enabling factors. Rather than simply shipping a finished product, we believe that the fact that the assembly and testing procedures took place entirely on location ensures a much greater transfer of knowledge, and the possibility for this knowledge to be passed on. In addition to being able to fabricate further systems, the ability to adjust, improve and repair such a system is enormously enhanced by the from-ground construction approach.

The estimated material costs (excluding machining and personnel) for this system given in euros are the following: plastic for the rings, 3000; magnets, 5000; 3D prints, 200; portable cart components, 500; glue, 1000; nuts/bolts/rods, 300; wire, 50. The Red Pitaya spectrometer and DAC boards can be put together for approximately 1000 and the gradient amplifier for about 2000, and the RF amplifier was purchased for about 100, although higher power would be necessary for imaging larger objects.

During a typical TSE sequence we estimate that the total power is about 120 W for the system, and about 40 W for the acquisition computer. We have run the gradient amplifiers off batteries. The RF amplifier could certainly be run from batteries, but we have not yet done so.

As outlined in the introduction, we had only two weeks to complete the build, and so the decision was taken to ship most of the materials from the Netherlands. With more time, we could certainly have investigated the possibilities of local manufacture of different components. It would have been particularly interesting to see the capabilities of local CNC engineering companies to produce the plastic formers for the magnet. We would anticipate that 3D printing facilities are more widespread, but the ability to order electronic components, and even relatively simple supplies such as copper wire, is highly variable between different countries. Overall, our aim is that the system described in this manuscript may now serve as a local benchmark for reproduction and eventual dissemination.

After construction this particular system is being used for training students about the basics of MRI. The system continues to perform well, and there are continuous updates available on the MaRCoS slack channels, which can be easily downloaded. Its ultimate use in any clinical studies will depend upon appropriate regulatory approval, and several different avenues are being explored to achieve this.

There are many additional factors that intersect the capacity requited to perform such a build, and the future enablement of sustainable education, medical applications and potential commercialization. In terms of education, this build was performed within a university school of engineering, led by a dean with an engineering PhD background in low-field MRI. The capacity building required to create the low-field engineering laboratory, support administration and personnel, and necessary outfit tools and testing equipment were supported under capacity building opportunities that parallel research projects through the Fogarty International Center at NIH; in addition, linking the laboratory capacity building with an ongoing hydrocephalus trial in Uganda provides a pathway towards future human medical evaluation over the coming years. Although academic programs are important for education, research and workforce development, we feel strongly that government partnership is critical if disruptive technologies such as this can intercalate into the regulatory, policy, medical and commercial ecosystem of a low- or middle-income country. Nevertheless, despite all of the funding, support and organization that went into getting us to this point, there are very substantial challenges that remain to successfully bring such a technology to the point of regulatory approval, health-care evaluation and commercial dissemination. These challenges are heightened within the largely unexplored terrain of open-source technology such as this. We suggest that this build is a clear demonstration of what is now possible with low-field MRI today, and that better coordination between government and research agencies could enhance the dissemination of this technology into the places in the world where the vast majority of people who need such imaging currently do not have access.

ACKNOWLEDGEMENTS

This work was funded by the National Institutes of Health (2R01HD085853), the Dutch Science Foundation (NWO–WOTRO joint SDG research program W 07.303.101, Stevin Prize 14997) and the European Research Council (Horizon 2020 ERC Advanced PASMAR 101021218).

ORCID

Andrew Webb https://orcid.org/0000-0003-4045-9732

REFERENCES

1. Ogbole GI, Adeyomoye AO, Badu-Peprah A, Mensah Y, Nzeh DA. Survey of magnetic resonance imaging availability in West Africa. *Pan Afr Med J*. 2018;30:240. doi:10.11604/pamj.2018.30.240.14000
2. Anazodo UC, Ng JJ, Ehiogu B, et al. A framework for advancing sustainable MRI access in Africa. *NMR Biomed*. 2023;36(3):e4846. doi:10.1002/nbm.4846
3. Geethanath S, Vaughan JT Jr. Accessible magnetic resonance imaging: a review. *J Magn Reson Imaging*. 2019;49(7):e65-e77. doi:10.1002/jmri.26638
4. *Local Production and Technology Transfer to Increase Access to Medical Devices—Addressing the Barriers and Challenges in Low- and Middle-Income Countries*. World Health Organization; 2012.
5. *Towards Improving Access to Medical Devices through Local Production. Phase II: Report of a Case Study in Four Sub-Saharan Countries*. World Health Organization; 2016.
6. Obungoloch J, Harper JR, Consevage S, et al. Design of a sustainable prepolarizing magnetic resonance imaging system for infant hydrocephalus. *Magn Reson Mater Phys Biol Med*. 2018;31(5):665-676. doi:10.1007/s10334-018-0683-y
7. O'Reilly T, Teeuwisse WM, de Gans D, Koolstra K, Webb AG. In vivo 3D brain and extremity MRI at 50 mT using a permanent magnet Halbach array. *Magn Reson Med*. 2021;85(1):495-505. doi:10.1002/mrm.28396
8. Guallart-Naval T, O'Reilly T, Algarin JM, et al. Benchmarking the performance of a low-cost magnetic resonance control system at multiple sites in the open MaRCoS community. *NMR Biomed*. 2023;36(1):e4825. doi:10.1002/nbm.4825
9. Dewan MC, Rattani A, Mekary R, et al. Global hydrocephalus epidemiology and incidence: systematic review and meta-analysis. *J Neurosurg*. 2018;1:1-15. doi:10.3171/2017.10.JNS17439
10. de Vos B, Parsa J, Abdulrazaq Z, et al. Design, characterisation and performance of an improved portable and sustainable low-field MRI system. *Front Phys*. 2021;9:701157.
11. Guallart-Naval T, Algarin JM, Pellicer-Guridi R, et al. Portable magnetic resonance imaging of patients indoors, outdoors and at home. *Sci Rep*. 2022;12(1):13147. doi:10.1038/s41598-022-17472-w
12. Han H, Moritz R, Oberacker E, Waiczies H, Niendorf T, Winter L. Open source 3D multipurpose measurement system with submillimetre fidelity and first application in magnetic resonance. *Sci Rep*. 2017;7(1):13452. doi:10.1038/s41598-017-13824-z
13. https://github.com/LUMC-LowFieldMRI/GradientAmplifier

14. O'Reilly T, Teeuwisse WM, Webb AG. Three-dimensional MRI in a homogenous 27 cm diameter bore Halbach array magnet. *J Magn Reson*. 2019;307:106578. doi:10.1016/j.jmr.2019.106578
15. de Vos B, Fuchs P, O'Reilly T, Webb A, Remis R. Gradient coil design and realization for a Halbach-based MRI system. *IEEE Trans Magn*. 2020;56(3):1-8. doi:10.1109/TMAG.2019.2958561
16. Cooley CZ, McDaniel PC, Stockmann JP, et al. A portable scanner for magnetic resonance imaging of the brain. *Nat Biomed Eng*. 2021;5(3):229-239. doi:10.1038/s41551-020-00641-5
17. https://github.com/LUMC-LowFieldMRI/GradientDesignTool
18. https://github.com/yvives/PhysioMRI_GUI
19. https://github.com/vnegnev/marcos_extras/wiki
20. Layton KJ, Kroboth S, Jia F, et al. Pulseq: a rapid and hardware-independent pulse sequence prototyping framework. *Magn Reson Med*. 2017;77(4):1544-1552. doi:10.1002/mrm.26235
21. Ravi KS, Geethanath S, Vaughan JT Jr. PyPulseq: a Python package for MRI pulse sequence design. *J Open Source Softw*. 2019;4(42):1725. doi:10.21105/joss.01725
22. Ravi KS, Potdar S, Poojar P, et al. Pulseq-graphical programming interface: open source visual environment for prototyping pulse sequences and integrated magnetic resonance imaging algorithm development. *Magn Reson Imaging*. 2018;52:9-15. doi:10.1016/j.mri.2018.03.008
23. https://github.com/LUMC-LowFieldMRI/RFPA_1kW
24. Srinivas SA, Cauley SF, Stockmann JP, et al. External Dynamic Interference Estimation and Removal (EDITER) for low field MRI. *Magn Reson Med*. 2022;87(2):614-628. doi:10.1002/mrm.28992
25. Liu YL, Leong ATL, Zhao YJ, et al. A low-cost and shielding-free ultra-low-field brain MRI scanner. *Nat Commun*. 2021;12(1):7238. doi:10.1038/s41467-021-27317-1

SUPPORTING INFORMATION

Additional supporting information can be found online in the Supporting Information section at the end of this article.

How to cite this article: Obungoloch J, Muhumuza I, Teeuwisse W, et al. On-site construction of a point-of-care low-field MRI system in Africa. *NMR in Biomedicine*. 2023;36(7):e4917. doi:10.1002/nbm.4917